

BLUEPRINT – Rebuilding a Legacy: Multimodal Retrieval for Complex Engineering Drawings and Documents

Ethan Seefried^{1,2} Ran Eldegaway¹ Sanjay Das¹ Nathaniel Blanchard² Tirthankar Ghosal¹

¹Oak Ridge National Laboratory, Oak Ridge, Tennessee

²Colorado State University, Fort Collins, Colorado

seefriedej@ornl.gov, ghosalt@ornl.gov

Abstract

Decades of engineering drawings and technical records remain locked in legacy archives with inconsistent or missing metadata, making retrieval difficult and often manual. We present BLUEPRINT, a layout-aware multimodal retrieval system designed for large-scale engineering repositories. BLUEPRINT detects canonical drawing regions, applies region-restricted VLM-based OCR, normalizes identifiers (e.g., DWG, part, facility), and fuses lexical and dense retrieval with a lightweight region-level reranker. Deployed on ~770k unlabeled files, it automatically produces structured metadata suitable for cross-facility search.

We evaluate BLUEPRINT on a 5k-file benchmark with 350 expert-curated queries using pooled, graded (0/1/2) relevance judgments. **BLUEPRINT delivers a 10.1% absolute gain in Success@3 and an 18.9% relative improvement in nDCG3 over the strongest vision-language baseline**, consistently outperforming across vision, text, and multimodal intents. Oracle ablations reveal substantial headroom under perfect region detection and OCR. We release all queries, runs, annotations, and code to facilitate reproducible evaluation on legacy engineering archives.

1. Introduction

Engineering organizations rely on diagrams, drawings, and linked documentation to design, operate, and maintain complex systems [47, 49]. Over decades, these assets accumulate across heterogeneous and siloed repositories (e.g., shared drives, PLM/EDRM systems, vendor portals), with idiosyncratic authoring styles and inconsistent conventions [68]. As sites modernize digital infrastructure and senior experts retire, critical knowledge risks becoming inaccessible [8, 10, 16, 24, 44, 57]. Fully re-cataloging legacy archives would require annotating hundreds of thousands of files, costly, slow, and error-prone, making scalable *retrieval*

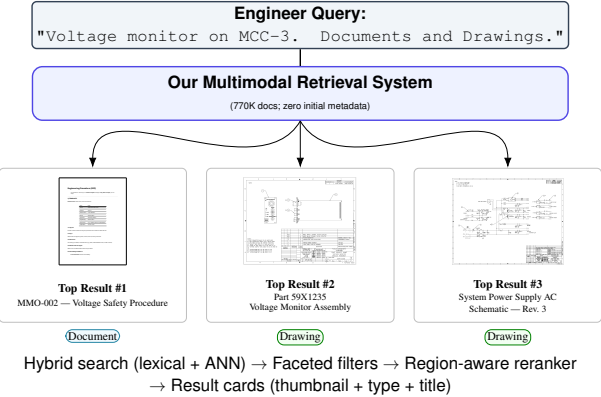


Figure 1. BLUEPRINT processes an engineer’s natural-language query and returns multimodal results across drawings, schematics, and procedural documents.

rather than re-labeling the core challenge.

Legacy corpora are heterogeneous in format (vector CAD, raster scans, TIFF/PDF, mixed-mode), quality (low-resolution scans, skew, bleed-through), and metadata (often missing or unreliable). Collections are inherently *multimodal*: visual drawings co-exist with policies, procedures, and narrative reports. Engineers query in text, but evidence often resides in visual regions such as title blocks, revision tables, or symbols. OCR noise, domain abbreviations, and near-duplicate revisions further complicate retrieval [7, 46]. These constraints motivate systems that fuse sparse textual signals with layout- and region-aware visual cues for robust, scalable retrieval over engineering documents.

We propose BLUEPRINT: Multimodal Retrieval for Engineering Archives, a framework that unifies computer vision and NLP for legacy engineering corpora. A lightweight *modality router* sends each file down a vision-first path (drawings, scans) or a text-first path (policies, procedures). On the vision path, the system detects layout regions (e.g., title block, revisions, parts list), applies region-restricted

OCR, and parses identifiers into structured metadata (e.g., drawing number, revision, facility tags, parts-list entries). On the text path, BLUEPRINT extracts key entities and section-level structure from procedural documents. These signals are fused into a joint embedding and indexed in a *hybrid* sparse+dense store. At query time, the system retrieves candidates via hybrid search and applies a lightweight reranker that promotes region-supported hits. The result is an efficient, end-to-end multimodal retrieval pipeline resilient to OCR noise, sparse text, and heterogeneous formats.

On a 5k-file benchmark with 375 mixed-modality queries, BLUEPRINT delivers state-of-the-art retrieval performance, with $\text{Success}@3 = 0.715 \pm 0.150$ and $nDCG@3 = 0.626 \pm 0.146$, achieving $\approx 10\%$ absolute gains over the strongest VLM baseline. At ≈ 9.7 s/file end-to-end throughput, BLUEPRINT is also the fastest. Pairwise LLM-as-judge comparisons show a 72.88% win rate against leading VLMs.

Our main contributions are:

- We introduce BLUEPRINT, an end-to-end system that integrates region detection, region-restricted VLM OCR, identifier normalization, and hybrid sparse+dense retrieval with a lightweight region-level reranker. Deployed at scale over hundreds of thousands of unlabeled engineering files, BLUEPRINT enables accurate cross-modal search across drawings, schematics, and technical documents.
- On a curated benchmark of 375 queries, BLUEPRINT consistently outperforms all vision-language baselines, delivering clear improvements in retrieval quality. This demonstrates that task-specific pipelines (e.g., YOLO + VLM OCR, LLM document routing) outperform general-purpose large VLMs such as LLaVA, Pixtral, and PaLI-Gemma.
- Region-level extraction substantially boosts retrieval accuracy, hybrid sparse+dense search outperforms single-modality retrieval, and OCR/box ablations reveal further headroom from improved layout understanding.
- We also contribute a graded relevance benchmark evaluated with three independent LLM judges and validated by human experts. BLUEPRINT achieves a strong win rate against all baselines and establishes a scalable evaluation protocol for large engineering-document collections.

2. Related Work

Document Retrieval Systems. Early retrieval systems relied on probabilistic and vector-space models [14, 15], with tf-idf and BM25 establishing strong lexical baselines [19, 56]. Classic improvements, including Rocchio-style relevance feedback [58] and inverted-index optimizations [6], enabled efficient keyword search at scale. Learning-to-rank approaches (RankSVM, LambdaMART) [9, 11] introduced supervised ranking over hand-crafted features.

Dense retrieval emerged with neural encoders such as DPR [32], which map queries and passages into a shared em-

bedding space for MIPS search with FAISS [31]. Subsequent work improved negative mining, cross-encoder distillation [22, 54], and late-interaction architectures such as ColBERT [38, 59]. LLM-based retrieval extends these ideas to text-generation settings, including RAG [3, 40], reranking [64], and zero-shot retrieval [60, 72]. However, these systems remain text-centric and degrade in symbol-heavy, OCR-noisy domains like engineering drawings.

Multimodal Retrieval for Technical Archives. Vision–language pretraining enables cross-modal matching through joint contrastive embeddings, as in CLIP/ALIGN [29, 55], which perform strongly on natural-image retrieval benchmarks such as COCO, Flickr30K, and VirTex [17, 41, 53]. Document-understanding models—LayoutLM, DocFormer, LayoutLLM [2, 23, 43, 70, 71]—fuse OCR text, layout structure, and appearance, showing strong results on FUNSD, DocLayNet, PubTables-1M, InfographicVQA, and ICDAR tasks [21, 28, 45, 52, 62]. These datasets assume relatively regular layouts and reliable OCR, which break down in legacy engineering archives.

Prior work in technical-domain retrieval targets scientific figure search [61], educational diagrams, or CAD retrieval, but engineering repositories pose additional challenges due to symbol-heavy layouts, facility-specific conventions, and the need for text–visual co-retrieval (e.g., retrieving both a safety policy and its referenced schematic). General VLMs (GPT-4V, LLaVA, Pixtral, Gemma-2) [1, 12, 20, 42, 65, 74] process pages holistically but struggle to recover schema-specific fields such as drawing numbers or revision identifiers. Traditional pipelines rely on OCR or detect–then–extract models [33, 48, 63, 66, 73], while OCR-free approaches (Donut, Florence-2) [35–37, 39, 69] still underperform on irregular schematics. BLUEPRINT closes this gap via region detection, VLM-OCR, structured parsing, and unified BM25+ANN indexing for schema-precise cross-modal retrieval at archive scale.

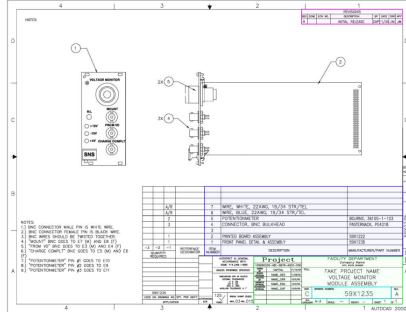
Evaluation of Retrieval Systems. IR evaluation typically uses pooled judging [67], graded relevance [26, 27], and multimodal benchmarks such as Flickr30K and COCO [41, 53]. Engineering queries lack ground-truth pairs, motivating pooled graded assessment. LLM-as-judge protocols [18, 75] offer scalability but require validation. We adopt a pooled 0/1/2 scheme judged by three independent LLMs (GPT-5 [50], LLaMA-3.2 [20], Mistral-7B [30]) with human auditing via Cohen’s κ and Kendall’s τ .

3. Dataset

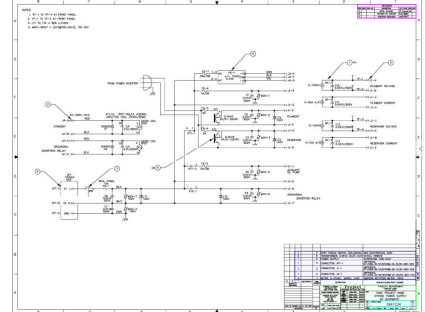
Our dataset consists of 770,000 unique files from a legacy document management system. Files contained limited or no metadata and spanned diverse formats: images, engineering drawings, textual documents, videos, and compressed archives. Since our goal is cross-modal retrieval between technical drawings and procedural documentation, we fil-



(a) Procedure document.



(b) Assembly drawing.



(c) Electrical schematic.

Figure 2. Representative samples: (a) policy/procedure with structured text, (b) assembly drawing with parts list and annotations, (c) electrical schematic with connection diagrams. Despite facility-specific conventions and missing regions in some drawings, common metadata areas (title block, drawing number, parts list, revisions) enable structured, layout-aware extraction for retrieval.

Table 1. File type distribution in the original dataset before and after filtering.

File Type	Count	Percent (%)	Extensions
Document	327,303	45.01	.pdf, .docx
Image	196,260	26.99	.jpg, .tiff
Other	195,206	26.85	.cad, .sldprt
Archive	7,392	1.02	.zip, .tar
Video	930	0.13	.mp4, .mov
Audio	28	0.00	.mp3, .wav
Engineering Drawings	166,125	29.72	.pdf, .sldprt
Documents	392,801	70.28	.pdf, .docx

tered for policies, procedures, and engineering drawings, yielding 558,926 unlabeled files.

3.1. File Types

Left with 558,926 unlabeled files, we primarily cared about 2 overarching categories of files: documents, and engineering drawings. Table 1 displays the initial dataset before metadata extraction.

Documents. The primary textual materials of interest were organizational *policies* and *procedures*. However, the legacy database also included a range of unrelated files such as images, videos, audio recordings, and archives. Document formatting was inconsistent across facilities, though most were stored as PDF or Microsoft Word files. In total, 392,801 documents were retained. Figure 2a illustrates an example procedure document, where the document should be templated.

Engineering Drawings. Engineering drawings in the dataset originated from multiple *anonymous facilities*, each employing distinct design conventions and labeling schemes. **Drawings from Facility A use metric units and DIN standards, while Facility B follows ANSI conventions, yet our retrieval system must handle both without facility-**

specific customization. As a result, no unified structure existed for extracting information. The drawings spanned a wide spectrum, from small parts to complete assemblies and electrical schematics, and appeared under various file extensions (e.g., PDF, CAD, etc.). In total, 392,801 documents were retained. Figures 2b, and 2c show example engineering diagrams and schematics that are related to each other.

3.2. Annotations

Test Sets. To support model development and evaluation, we constructed two manually annotated subsets from the 770,000 unlabeled files. First, a 500-sample pilot set (211 drawings, 289 documents) was randomly selected and labeled using a lightweight `matplotlib`-based interface; this enabled rapid iteration and early model selection. Building on this, we assembled a higher-confidence *golden test set* of 1,500 new, non-overlapping files, sampled at a balanced 50/50 split (750 drawings, 750 documents) and annotated using the same procedure. The golden set serves as the primary benchmark for comparing tuned models.

Metadata Extraction. We annotated the 750-image golden test set using CVAT [13], producing YOLO-format bounding boxes for four standardized metadata regions commonly found in engineering drawings: *drawing number*, *data block*, *parts list*, and *revisions block*. Of the 750 drawings, 749 were successfully labeled. These regions were selected because they contain structured identifiers critical for indexing and retrieval.

Table 2 reports the train/val/test splits along with counts of each metadata region. Coverage is high across all splits, with only a handful of drawings missing individual fields. Splits were assigned randomly with the constraint that each subset contained a representative number of *parts lists*, ensuring balanced supervision for this key region. This labeled set provides a reliable foundation for training and evaluating region detectors whose accuracy directly influences downstream retrieval quality.

Table 2. Summary of dataset splits showing the number of drawings and labeled metadata regions (parts list, data block, drawing number, and revisions block) across train, validation, and test sets.

Split	Files	Parts	Data	Drw.	Rev.
Train	500	232	495	496	455
Val	150	70	150	150	150
Test	99	45	98	98	89

Dataset availability. The operational corpus contains sensitive engineering records and cannot be released. We provide full code, prompts, normalization rules, index configurations, seeds. To enable reproducibility, we will release an independent 5k+ benchmark of unrestricted engineering documents, with the same queries and relevance judgments, which will serve as the held-out test set for an upcoming shared task. A larger 50k+ open dataset of annotated engineering diagrams (components, relationships, multimodal tasks) is also in development and will be released with baselines, culminating in a community shared task.

4. BLUEPRINT

We employ a 2 stage pipeline beginning with document routing (document or drawing), before splitting into an NLP pipeline and Vision pipeline, and combining into a multi-modal retrieval system. Figure 3 showcases the architecture.

4.1. Document Routing

We identify whether a file is an engineering drawing or a document using a zero-shot CLIP classifier [55] augmented with lightweight domain heuristics. Drawings typically contain strong borders ($b^{(i)}$), dense edges ($edge^{(i)}$), and long straight lines ($lines^{(i)}$); these cues form a heuristic score $h^{(i)}$. We additionally include a CAD prior $c^{(i)}$ based on extensions such as `.dwg` or `.sldprt`. Thus each file $F^{(i)}$ is represented by $(p_{\text{draw}}^{(i)}, h^{(i)}, c^{(i)})$, where $p_{\text{draw}}^{(i)}$ is the CLIP drawing probability.

To combine these signals, we fit a logistic regression on 500 manually labeled files, modeling $\text{logit } P(y^{(i)}=\text{drawing}) = \alpha + \beta_{\text{clip}} p_{\text{draw}}^{(i)} + \beta_{\text{heur}} h^{(i)} + \beta_{\text{cad}} c^{(i)} + \beta_{\text{int}} (p_{\text{draw}}^{(i)} h^{(i)})$. The learned coefficients show that CLIP is the dominant predictor ($\beta_{\text{clip}} \approx 5.91$), while a positive interaction term ($\beta_{\text{int}} \approx 2.21$) indicates that heuristics meaningfully reinforce CLIP when both agree; heuristics alone carry a small negative weight ($\beta_{\text{heur}} \approx -0.81$).

Empirically, this calibrated combination outperforms both CLIP alone and all heuristic-only baselines: CLIP+heuristics achieves 94.5% accuracy on the golden test set, improving drawing recall from 94.5% (CLIP) to 97.7% while also reducing false positives. This blend of semantic (CLIP) and structural (heuristic) cues yields a reliable routing signal for

downstream retrieval.

4.2. Vision Pipeline

Information Extraction. We localize metadata regions with a YOLOv8-S detector [63] trained on our annotations using a multi-task objective (DFL for box regression, CLS, and IoU). On our benchmark it achieves 89.5% mAP@0.5:0.95 with 5.2 ms/image on an NVIDIA A100. The detector reliably finds four key regions: *drawing number*, *data block*, *parts list*, and *revisions block*, which anchor downstream extraction.

After localization, we apply a VLM OCR/IE module (“LLaMa-4”) to *each crop* with brief, field-aware prompts. Although the base model is not “lightweight,” the region-only setup (small crops, short prompts, 8-bit quantized inference, capped resolution) yields markedly lower latency than full-page passes while improving exact-field precision. Outputs are normalized and schema-validated before indexing.

4.3. NLP Pipeline

Document Parsing and Classification. After separating drawings from textual documents, we implemented an NLP pipeline to categorize and parse the 392,801 document files for downstream normalization and retrieval. Rather than serving as ground-truth labels, these categories provide operational routing for policy- and procedure-focused queries. We used GPT-4o-mini [51] to assign each document to one of three governance-relevant classes: *policy*, *procedure*, or *other*, via a prompt defining organizational rules (policies), step-wise instructions (procedures), and all remaining technical or administrative documents. Only the first 5 pages (or 8,000 characters) were analyzed to balance accuracy with throughput.

Document text was then extracted using a hybrid pipeline: for PDFs, we first applied EasyOCR [25] to rendered pages and fell back to the native text layer (PyMuPDF [4]) when OCR returned no content; DOCX files used python-docx, and other image-based documents were processed directly with EasyOCR. The resulting text was normalized (section headers, step lists, references, units) and embedded using the Nemotron-based textual encoder.

4.4. Unified Retrieval

Shared vector space. All documents and drawing regions are embedded into a common vector space $\mathbf{z}_d \in \mathbb{R}^m$ that fuses text-derived signals (policy/procedure OCR and region-level OCR) with layout-aware features. We use the NEMOTRON-7B embedding model [5] to obtain a normalized textual embedding \mathbf{t}_d , and we extract a complementary layout/region feature vector \mathbf{r}_d . We learn lightweight projection layers W_t and W_r and form the final document embedding as $\mathbf{z}_d = \text{norm}(W_t \mathbf{t}_d \oplus W_r \mathbf{r}_d)$, where \oplus denotes concatenation and $\text{norm}(\cdot)$ is ℓ_2 normalization. Queries are embedded purely from text using $\mathbf{z}_q = \text{norm}(W_q \mathbf{t}_q)$.

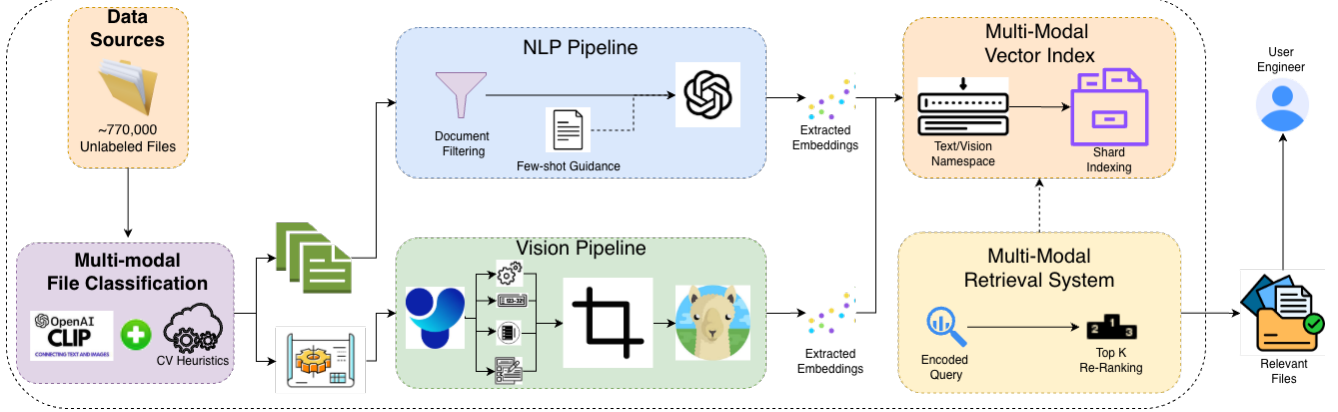


Figure 3. Our multimodal retrieval system processes $\sim 770k$ unlabeled technical documents through parallel NLP and Vision pipelines. Documents are first routed via zero-shot multimodal classification (CLIP + domain-specific CV heuristics). The NLP pipeline performs document filtering and text embedding extraction, while the Vision pipeline applies preprocessing, spatial cropping, and visual encoding. Both modalities populate a unified multimodal vector index with sharded storage for scalability. At query time, encoded queries retrieve candidates from the index and a re-ranking stage returns the top- K most relevant documents, enabling robust search over heterogeneous document types without manual metadata.

Queries We evaluate on $|\mathcal{Q}| = 375$ natural-language queries crafted with a domain expert and stratified by intent: $\mathcal{Q} = \mathcal{Q}_{\text{draw}} \cup \mathcal{Q}_{\text{doc}} \cup \mathcal{Q}_{\text{xmod}}$ with $|\mathcal{Q}_{\text{draw}}| = 150$, $|\mathcal{Q}_{\text{doc}}| = 150$, and $|\mathcal{Q}_{\text{xmod}}| = 75$. These cover drawing-centric lookups ($\mathcal{Q}_{\text{draw}}$), policy/procedure lookups (\mathcal{Q}_{doc}), and cross-modal queries that should return both drawings and documents ($\mathcal{Q}_{\text{xmod}}$).

Query form and normalization. Each query $q \in \mathcal{Q}$ is free text but can be viewed as a slot template $\phi(q) = \{\text{facility}, \text{asset/part}, \text{doc_type}, \text{constraints}\}$ when applicable (e.g., revision filters, date ranges). We apply light normalization to q (case folding; punctuation/whitespace canonicalization) prior to retrieval; this only affects matching and does not alter the text presented to judges.

Judging protocol. For each query q , systems return the top $k = 3$ items. Relevance is scored on a 3-point scale $\ell(q, d) \in \{0, 1, 2\}$. To scale evaluation across $\sim 770k$ documents, we use three independent LLM judges (GPT-5, Llama-3.2-11B-Vision, Mistral-7B), each scoring items in isolation to reduce cross-system bias. A small, stratified subset is reviewed by three human evaluators to validate agreement and resolve ambiguous cases.

Pooling and de-duplication. For fair recall estimation, we pool all systems’ top- k results per query, collapse near-duplicates (e.g., successive revisions of the same drawing), and judge the merged set. Real-world artifacts such as low-quality or partially unreadable scans are kept, while only truly corrupted files are excluded and tracked for coverage.

Examples. Drawing-centric ($q \in \mathcal{Q}_{\text{draw}}$): “Facility R8E8700 — voltage monitor on MCC-3; exclude revisions.”

Policy-centric ($q \in \mathcal{Q}_{\text{doc}}$): “Cylinder transport procedure for cryogenic tanks; pre-lift checklist.”

Multi-modal ($q \in \mathcal{Q}_{\text{xmod}}$): “Lockout/tagout policy and corresponding electrical schematic for Main Panel TG:CAB1800.”

Scoring and ranking. For each document $d \in C$, we compute a sparse retrieval score $s_{\text{sparse}}(d \mid q') = \text{BM25}(q', d)$ and a dense retrieval score $s_{\text{dense}}(d \mid q) = \cos(\mathbf{z}_q, \mathbf{z}_d)$, where q' is a rewritten or expanded query string used for BM25 and q is the original text used for dense embeddings. We fuse these with per-query z-score normalization, $\tilde{s}_*(d) = (s_*(d) - \mu_*(q))/\sigma_*(q)$, yielding $s_\lambda(d \mid q) = \lambda \tilde{s}_{\text{sparse}}(d) + (1 - \lambda) \tilde{s}_{\text{dense}}(d)$, where $\lambda \in [0, 1]$ is tuned on a held-out validation set (using a robust variance clamp for small $|C|$). A lightweight reranker then promotes region-consistent hits and penalizes revision mismatches: $s_{\text{final}}(d \mid q) = s_\lambda(d \mid q) + \alpha \text{match}_{\text{region}}(d, q) + \beta \text{consistency}_{\text{rev}}(d, q) - \gamma \mathbb{1}[\text{off-type}(d, q)]$. Here, $\text{match}_{\text{region}} \in \{0, 1\}$ activates when fields extracted from YOLO-detected regions (e.g., title block, parts list, or facility tag) satisfy query constraints, $\text{consistency}_{\text{rev}} \leq 0$ penalizes disallowed revisions, and $\gamma \geq 0$ optionally penalizes modality mismatches (e.g., drawing vs. document) when *Allowed types* are specified. Ties are resolved by normalized document recency (based on date metadata) and page quality (OCR confidence or image resolution). The top-ranked results are returned as $R_k(q) = \text{TopK}(\{(d, s_{\text{final}}(d \mid q)) : d \in C\}, k = 3)$.

5. Experiments

We evaluate BLUEPRINT, our multimodal retrieval framework, on a 5k subset randomly selected from the 558,926-

Table 3. Overall retrieval performance across 375 benchmark queries (150 vision, 150 NLP, 75 multi-modal). Each query contributes the top-3 results per system (≈ 6300 document-level judgments). Reported values are mean \pm 95% CI computed over query-level scores.

System	nDCG@3	MAP@3 (≥ 1)	MAP@3 (=2)	P@3	R@3	Succ@3
LLaMA 3.2 Vision	0.521 ± 0.248	0.497 ± 0.244	0.330 ± 0.256	0.342 ± 0.145	0.151 ± 0.052	0.623 ± 0.273
Llama 4 Scout 17B	0.519 ± 0.158	0.503 ± 0.156	0.327 ± 0.200	0.364 ± 0.096	0.137 ± 0.012	0.607 ± 0.178
LLaVA 1.6 Mistral 7B	0.400 ± 0.246	0.378 ± 0.236	0.193 ± 0.138	0.275 ± 0.154	0.109 ± 0.058	0.498 ± 0.290
PaliGemma 2	0.422 ± 0.240	0.395 ± 0.232	0.195 ± 0.169	0.307 ± 0.166	0.122 ± 0.051	0.533 ± 0.281
Pixtral 12B (2409)	0.502 ± 0.159	0.486 ± 0.153	0.314 ± 0.233	0.354 ± 0.114	0.131 ± 0.022	0.592 ± 0.186
BLUEPRINT (Ours)	0.626 ± 0.146	0.608 ± 0.147	0.407 ± 0.241	0.435 ± 0.091	0.222 ± 0.037	0.715 ± 0.150

document corpus in Section 3. Our study centers on 370 expert-crafted queries reflecting realistic operational needs. We assess: (i) **Retrieval performance** across heterogeneous technical documents (MAP@10, nDCG@10, Precision@10, Recall@10, Success@{1, 3}); (ii) **Cross-modal capability** (text→drawing and text→policy, plus mixed intents); and (iii) **Component importance** via ablations on routing, extraction quality, and embedding/fusion design. We compare against open-source end-to-end vision–language baselines operating on the same full-page renders.

5.1. Experimental Setup

Metrics. We use graded relevance (0/1/2) and report nDCG@3, MAP@3, Precision@3, Recall@3, and Success@{1, 3}. We normalize text (case/punctuation), collapse near-duplicate drawing revisions, and measure latency as seconds per file. For fair comparison, all systems operate on the same full-page render; VLM baselines score the page directly, while BLUEPRINT applies detect→crop→OCR/IE before indexing. Ranking uses a fused score $s(d | q) = \lambda s_{\text{sparse}} + (1 - \lambda)s_{\text{dense}}$ with per-query z-normalized dense scores and λ tuned on held-out queries. We report 95% bootstrap CIs, paired randomization tests by query bucket, and expert–LLM agreement (weighted κ , Kendall’s τ). Un-judgeable items are excluded, and coverage is reported.

Query set. We evaluate on **375 natural-language queries** crafted with a domain expert: 150 drawing-centric, 150 policy/procedure-centric, and 75 cross-modal (document+drawing). Each query is issued once per system; we collect top- k results with $k = 3$ unless stated otherwise. We report metrics per bucket and macro-averaged over all queries.

Evaluation protocol. To maximize coverage under limited human time and variable scan quality, we use an *LLM-as-judge* protocol as the primary relevance signal. For each query–system pair, the top- k results ($k = 3$) are graded on a 0/1/2 rubric over anonymized, randomized items. Near-duplicate pages are pooled and unjudgeable scans excluded. For *human auditing*, three raters label the top-1 result on a stratified subset of queries; we report quadratic Cohen’s κ_w

and Kendall’s τ between expert and LLM nDCG@3, with uncertainty from 10k bootstrap resamples. We additionally report head-to-head *win/lose/tie* rates using nDCG@1 with 95% CIs.

Baselines. We compare against end-to-end VLMs that score full-page renders without region crops or OCR pre-processing: **LLaMA 3.2 Vision** (pooled embedding cosine), **LLaVA 1.6 Mistral-7B** (embedding head; cross-attention tie-break), **PaliGemma 2** (pooled VL embeddings), **Pixtral-12B (2409)** (pooled embeddings or pairwise scoring), and **Llama 4 Scout 17B** (pooled similarity; pairwise fallback). We selected baselines that can be run locally to ensure reproducibility, fixed compute budgets, and consistent evaluation across the corpus.

5.2. Retrieval Performance

We evaluate retrieval quality using both ranking statistics (nDCG, MAP, Precision/Recall, Success) and pairwise win rates. All metrics are computed over 375 benchmark queries (150 vision, 150 NLP, and 75 multi-modal), each contributing the top-3 ranked results per system. For statistical evaluation, we use three independent LLMs: **GPT-5**, **Llama-3.2-Vision**, and **Mistral-7B**, as judges. These models were selected based on their strong performance in the Hugging-Face *LLM-as-Judge* leaderboard and were given identical grading prompts.

Table 3 reports the mean \pm 95% confidence intervals of the query-level scores. Across all metrics, BLUEPRINT achieves the highest performance, outperforming the next closest baselines (*Llama-4-Scout* and *Llama-3.2-Vision*) by roughly **10% absolute** in both Success@3 and nDCG@3. These gains indicate that BLUEPRINT not only ranks relevant documents higher but also returns at least one correct result within the top-3 for over 70% of queries.

Table 4 complements these aggregate statistics with *LLM-as-Judge* win-rates in a pairwise “1-vs-1” setting, comparing BLUEPRINT to every other system across 325 queries. BLUEPRINT is preferred in **72.9%** of head-to-head comparisons on average, while the strongest baseline, *Llama-4-Scout-17B*, attains only **38.3%**. A sensitivity analysis excluding the weakest baseline (*PaliGemma-2*) yields a consistent

win rate of 69.1%, confirming that the observed improvements are robust across evaluation setups.

5.3. Human Evaluation

To validate the reliability of our automated relevance assessments, we conducted a three-person human study consisting of one domain expert and two trained raters. All annotators used the same 3-point relevance scale (0/1/2) as the LLM-based judges and rated the top-1 result for a representative set of 50 queries (25 drawings, 15 NLP, 10 cross-modal). **Rater agreement.** Human inter-rater reliability is strong: pairwise quadratic Cohen’s κ ranges from 0.49–0.69, and the multi-rater Fleiss’ κ is **0.399**, indicating substantial consistency and establishing a stable human reference for evaluating retrieval quality. **Human vs. LLM agreement.** As shown in Table 5, expert consensus also exhibits positive agreement with the LLM ensemble used in our automated judging pipeline: across all overlapping items ($n = 295$), quadratic $\kappa_w = 0.31$ [0.19, 0.42], with comparable values for Drawings (0.35), Procedures (0.25), Cross-Modal (0.25), and Policies (0.24). Although conservative, the LLM judges remain directionally aligned with expert assessments, supporting their use at large scale where human labeling is infeasible. Overall, the human study shows that (i) human raters are internally consistent, (ii) LLM-based 0/1/2 judgments meaningfully track expert consensus, and (iii) **BLUEPRINT** remains the top-ranked system under both human and automated evaluation.

Table 4. LLM-as-judge results showing pairwise wins, losses, and ties against **BLUEPRINT** across 325 queries (150 vision, 150 NLP, 75 multi-modal). Win % is computed as wins/(wins+losses), with ties excluded.

System	Wins	Losses	Ties	Win %
LLaMA 3.2 Vision	263	645	104	28.96
Llama 4 Scout 17B	331	532	152	38.35
LLaVA 1.6 Mistral 7B	166	723	123	18.67
PaliGemma 2	117	800	108	12.76
Pixtral 12B	328	538	138	37.88
BLUEPRINT 17B (overall)	3238	1205	625	72.88[†]

[†] Sensitivity analysis excluding *PaliGemma* (an atypically low baseline) yields a **BLUEPRINT** win rate of 69.14%; the main table reports the all-systems result to avoid inflating performance due to a single weak model.

5.4. Ablation Studies

OCR Ablations. We ablate only the OCR stage while holding indexing, embeddings, reranking, and normalization fixed (Table 6). We compare Tesseract [34] and EasyOCR [25] with (i) *predicted* **BLUEPRINT** boxes, (ii) *oracle* (GT) boxes, and (iii) a *full-page* diagnostic; we also evaluate our **BLUEPRINT** VLM-OCR under the same box regimes. Relevance is judged by an LLM ensemble (GPT-5, LLaMA 3,

Table 5. Agreement between expert consensus and the LLM-ensemble on raw 0/1/2 relevance labels. Counts (n) refer to *items*, each query contributes one top-1 result per system, yielding 295 overlapping human+LLM annotations across the 50 human-evaluated queries. κ_w : quadratic-weighted Cohen’s kappa with bootstrap 95% CIs.

Bucket	n	κ_w (95% CI)
All	295	0.31 [0.19, 0.42]
Drawings	149	0.35 [0.12, 0.56]
Procedures	51	0.25 [0.07, 0.43]
Multi-Modal	59	0.25 [0.08, 0.44]
Policies	24	0.24 [-0.01, 0.51]

Phi-3.5) and reported as means averaged across judges (per-judge 95% CIs in the appendix).

Three takeaways emerge. (1) **Layout-aware OCR beats full-page OCR:** both Tesseract and EasyOCR drop substantially on full-page runs. (2) **Predicted boxes are competitive with oracle boxes for classic OCR**, indicating our detector reliably localizes informative regions. (3) **BLUEPRINT VLM-OCR is strongest overall:** with oracle boxes it achieves **0.699** nDCG@3, **0.675** MAP@3 (≥ 1), and **0.780** Succ@3; with predicted boxes it remains ahead of traditional engines (nDCG@3 **0.563**, Succ@3 **0.644**). These results underscore that accurate region proposals *and* a multimodal, drawing-aware OCR are both critical for retrieval in engineering archives.

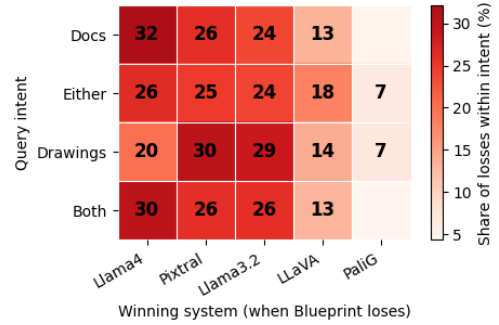


Figure 4. Heatmap showing which baselines win against **BLUEPRINT** across query intents. “Either” entries reflect queries where judges accept drawings or documents, and values show the percentage of losses per intent.

5.5. Error analysis

Across all pairwise comparisons where **BLUEPRINT** loses under the Llama-3 judge, the loss rate is highest for document-only queries (DOCS, 35.9%) and auto-generated queries (AUTO, 27.5%), and markedly lower for drawing-centric intents (DRAWINGS, 20.1%; BOTH, 19.2%). This matches our design goal: **BLUEPRINT** is specialized for engineering

Table 6. OCR ablations on **val/test** with LLM-as-judge (*GPT-5, LLaMA-3, Phi-3.5-mini*). We report top-3 retrieval metrics (nDCG@3, MAP@3, P@3, R@3, Succ@3) as *means across judges* (per-judge CIs in the appendix). All variants share identical indexing and reranking; only the OCR stage and region regime differ (traditional OCR vs. BLUEPRINT VLM-OCR, predicted boxes, oracle GT boxes, or full-page).

System Variant	nDCG@3	MAP@3 (≥ 1)	MAP@3 (=2)	P@3	R@3	Succ@3
Tesseract (Pred boxes)	0.532	0.525	0.427	0.353	0.582	0.582
Tesseract (Oracle boxes)	0.457	0.439	0.384	0.261	0.509	0.509
EasyOCR (Pred boxes)	0.525	0.513	0.440	0.323	0.573	0.573
EasyOCR (Oracle boxes)	0.390	0.373	0.304	0.235	0.442	0.442
Tesseract (Fullpage) <i>diag.</i>	0.208	0.197	0.128	0.108	0.240	0.240
EasyOCR (Fullpage) <i>diag.</i>	0.287	0.270	0.181	0.159	0.338	0.338
BLUEPRINT (Pred boxes, VLM-OCR)	0.563	0.539	0.458	0.313	0.644	0.644
BLUEPRINT (Oracle boxes , VLM-OCR)	0.699	0.675	0.601	0.401	0.780	0.780

drawings and trades some performance on generic document retrieval. When it does lose, the winners are typically large full-page VLMs (e.g., Llama-4-Scout-17B, Pixtral-12B), with smaller models rarely outperforming it. Qualitative inspection highlights three recurring failure modes: modality routing errors (retrieving drawings instead of procedures), region/OCR misses on fine-grained attributes, and cross-document reasoning failures, which suggest future improvements in document routing, region-level OCR, and document–drawing linkage. Figure 4 displays a heatmap of loss percentage broken down by query type.

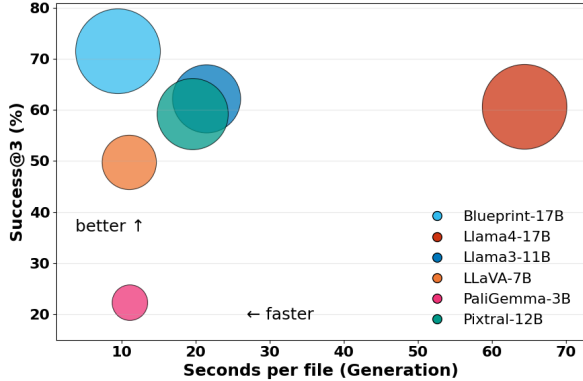


Figure 5. Latency–accuracy trade-off across systems. BLUEPRINT attains the fastest end-to-end processing time (≈ 9.46 s/file) and the highest retrieval accuracy (Succ@3 = 71.5%), outperforming all vision–language baselines. Bubble size indicates parameter count.

6. Discussion

Key Insights. BLUEPRINT delivers the best combination of accuracy, reliability, and efficiency across our full 770k-document environment. Against the strongest baseline (Llama-4-Scout-17B), paired bootstrap tests show large, statistically significant improvements for engineering-drawing retrieval (e.g., nDCG@3: $\Delta = +0.26$, 95% CI [0.22, 0.31]; Succ@3: $\Delta = +0.27$, CI [0.22, 0.32]). For multimodal

queries the systems are statistically tied, and for document-only queries Scout shows a small, non-significant advantage.

Despite using a multi-stage pipeline, BLUEPRINT is the fastest system, achieving 9.46 s/file versus 64.36 s/file for Llama-4-Scout and 19.6–21.5 s/file for other VLMs, as seen in Figure 5. It also achieves the highest Success@3 (71.5%), substantially above the strongest baseline (60.7%). Overall, BLUEPRINT provides both statistical gains and operational advantages, especially for drawing-centric search scenarios that dominate real engineering workflows.

Limitations. Our metadata schema was chosen with expert engineers as the most critical fields for retrieval/compliance, but it is not exhaustive; site-specific cues (e.g., vendor callouts, atypical “as-built” notes) may be missed. We also assume readable scans and identifiable regions, so severe degradation or nonstandard title blocks can reduce fidelity. The reranker currently handles a small set of constraints (facility/tag/revision) and does not yet model richer cross-document relations.

7. Conclusions

We presented BLUEPRINT, a layout-aware multimodal retrieval framework for engineering documents and drawings. By coupling region detection, VLM-based OCR, and normalized text in a unified embedding space, BLUEPRINT delivers state-of-the-art performance on 375 graded queries (e.g., **0.626** nDCG@3, **0.715** Succ@3), outperforming strong open-source VLM baselines. The results highlight the value of structured, region-aware extraction for technical corpora.

The approach generalizes to diagram-heavy domains such as BIM/architecture, aerospace schematics, and technical manuals, enabling applications in cross-modal search, compliance, maintenance, and archive modernization.

Future Work. We will extend extraction to relation graphs, introduce lightweight rerankers for hard negatives, and further improve robustness to degraded scans and multilingual symbols. In parallel, we plan to release a cross-domain benchmark and organize a community shared task.

References

[1] Pravesh Agrawal, Szymon Antoniak, Emma Bou Hanna, Baptiste Bout, Devendra Chaplot, Jessica Chudnovsky, Diogo Costa, Baudouin De Monicault, Saurabh Garg, Theophile Gervet, et al. Pixtral 12b. *arXiv preprint arXiv:2410.07073*, 2024. [2](#)

[2] Srikanth Appalaraju, Bhavan Jasani, Bhargava Urala Kota, Yusheng Xie, and R Manmatha. Docformer: End-to-end transformer for document understanding. In *Proceedings of the IEEE/CVF international conference on computer vision*, pages 993–1003, 2021. [2](#)

[3] Muhammad Arslan, Hussam Ghanem, Saba Munawar, and Christophe Cruz. A survey on rag with llms. *Procedia computer science*, 246:3781–3790, 2024. [2](#)

[4] Inc. Artifex Software. Mupdf: A lightweight pdf, xps, and ebook renderer. <https://mupdf.com/>, 2025. [4](#)

[5] Yauhen Babakhin, Radek Osmulski, Ronay Ak, Gabriel Moreira, Mengyao Xu, Benedikt Schifferer, Bo Liu, and Even Oldridge. Llama-embed-nemotron-8b: A universal text embedding model for multilingual and cross-lingual tasks, 2025. [4](#)

[6] Dmitry Baranchuk, Artem Babenko, and Yury Malkov. Revisiting the inverted indices for billion-scale approximate nearest neighbors, 2018. [2](#)

[7] Guilherme Torresan Bazzo, Gustavo Acauan Lorentz, Danny Suarez Vargas, and Viviane P Moreira. Assessing the impact of ocr errors in information retrieval. In *European Conference on Information Retrieval*, pages 102–109. Springer, 2020. [1](#)

[8] Nikki Bell. Mitigating the loss of critical knowledge. In *Safety and Reliability*, pages 61–78. Taylor & Francis, 2014. [1](#)

[9] Christopher JC Burges. From ranknet to lambdarank to lambdamart: An overview. *Learning*, 11(23-581):81, 2010. [2](#)

[10] Anne Burmeister and Jürgen Deller. Knowledge retention from older and retiring workers: What do we know, and where do we go from here? *Work, Aging and Retirement*, 2(2):87–104, 2016. [1](#)

[11] Yunbo Cao, Jun Xu, Tie-Yan Liu, Hang Li, Yalou Huang, and Hsiao-Wuen Hon. Adapting ranking svm to document retrieval. In *Proceedings of the 29th annual international ACM SIGIR conference on Research and development in information retrieval*, pages 186–193, 2006. [2](#)

[12] Xiangxiang Chu, Jianlin Su, Bo Zhang, and Chunhua Shen. Visionllama: A unified llama backbone for vision tasks. In *European Conference on Computer Vision*, pages 1–18. Springer, 2024. [2](#)

[13] Computer Vision Annotation Tool (CVAT) developers. Computer vision annotation tool (cvat), 2023. [3](#)

[14] WB Croft. Document retrieval system. *Information Technology*, 2:1–21, 1983. [2](#)

[15] W Bruce Croft and Roger H Thompson. I3r: A new approach to the design of document retrieval systems. *Journal of the american society for information science*, 38(6):389–404, 1987. [2](#)

[16] Abdelkader Daghfous, Omar Belkhodja, and Linda C. Angell. Understanding and managing knowledge loss. *Journal of knowledge management*, 17(5):639–660, 2013. [1](#)

[17] Karan Desai and Justin Johnson. Virtex: Learning visual representations from textual annotations, 2021. [2](#)

[18] Yann Dubois, Balázs Galambosi, Percy Liang, and Tatsumori B. Hashimoto. Length-controlled alpaca-eval: A simple way to debias automatic evaluators, 2025. [2](#)

[19] Mathias Géry and Christine Largeron. Bm25t: a bm25 extension for focused information retrieval. *Knowledge and information systems*, 32(1):217–241, 2012. [2](#)

[20] Aaron Grattafiori, Abhimanyu Dubey, Abhinav Jauhri, Abhinav Pandey, Abhishek Kadian, Ahmad Al-Dahle, Aiesha Letman, Akhil Mathur, Alan Schelten, Alex Vaughan, et al. The llama 3 herd of models. *arXiv preprint arXiv:2407.21783*, 2024. [2](#)

[21] Adam W Harley, Alex Ufkes, and Konstantinos G Derpanis. Evaluation of deep convolutional nets for document image classification and retrieval. In *International Conference on Document Analysis and Recognition (ICDAR)*, 2015. [2](#)

[22] Sebastian Hofstätter, Sheng-Chieh Lin, Jheng-Hong Yang, Jimmy Lin, and Allan Hanbury. Efficiently teaching an effective dense retriever with balanced topic aware sampling, 2021. [2](#)

[23] Yupan Huang, Tengchao Lv, Lei Cui, Yutong Lu, and Furu Wei. Layoutlmv3: Pre-training for document ai with unified text and image masking. In *Proceedings of the 30th ACM international conference on multimedia*, pages 4083–4091, 2022. [2](#)

[24] Gregory Huet, Christopher A McMahon, Florence Sellini, Stephen J Culley, and Clément Fortin. Knowledge loss in design reviews. In *Advances in Integrated Design and Manufacturing in Mechanical Engineering II*, pages 277–291. Springer, 2007. [1](#)

[25] JaidedAI. Easyocr: Ready-to-use ocr with 80+ supported languages. <https://github.com/JaidedAI/EasyOCR>, 2020. Accessed 2025-11-03. [4, 7](#)

[26] K Järvelin. & kekäläinen, j. cumulated gain-based evaluation of ir techniques. *ACM Transactions on Information Systems*, 20, 2002. [2](#)

[27] Kalervo Järvelin and Jaana Kekäläinen. Ir evaluation methods for retrieving highly relevant documents. *SIGIR Forum*, 51(2):243–250, 2017. [2](#)

[28] Guillaume Jaume, Hazim Kemal Ekenel, and Jean-Philippe Thiran. Funsd: A dataset for form understanding in noisy scanned documents, 2019. [2](#)

[29] Chao Jia, Yinfei Yang, Ye Xia, Yi-Ting Chen, Zarana Parekh, Hieu Pham, Quoc V. Le, Yunhsuan Sung, Zhen Li, and Tom Duerig. Scaling up visual and vision-language representation learning with noisy text supervision, 2021. [2](#)

[30] Albert Q. Jiang, Alexandre Sablayrolles, Arthur Mensch, Chris Bamford, Devendra Singh Chaplot, Diego de las Casas, Florian Bressand, Gianna Lengyel, Guillaume Lample, Lucile Saulnier, Lélio Renard Lavaud, Marie-Anne Lachaux, Pierre Stock, Teven Le Scao, Thibaut Lavril, Thomas Wang, Timothée Lacroix, and William El Sayed. Mistral 7b, 2023. [2](#)

[31] Jeff Johnson, Matthijs Douze, and Hervé Jégou. Billion-scale similarity search with gpus, 2017. [2](#)

[32] Vladimir Karpukhin, Barlas Oğuz, Sewon Min, Patrick Lewis, Ledell Wu, Sergey Edunov, Danqi Chen, and Wen tau Yih.

Dense passage retrieval for open-domain question answering, 2020. [2](#)

[33] Alexey Kashevnik, Nikolay Shilov, Nikolay Teslya, Fudail Hasan, Andrey Kitenko, Veronika Dukareva, Marat Abdurakhimov, Alexander Zingarevich, and Dmitry Blokhin. An approach to engineering drawing organization: Title block detection and processing. *IEEE Access*, pages 1–1, 2023. [2](#)

[34] Anthony Kay. Tesseract: an open-source optical character recognition engine. *Linux Journal*, 2007(159):2, 2007. [7](#)

[35] Muhammad Tayyab Khan, Lequn Chen, Ye Han Ng, Wenhe Feng, Nicholas Yew Jin Tan, and Seung Ki Moon. Fine-tuning vision-language model for automated engineering drawing information extraction. *arXiv preprint arXiv:2411.03707*, 2024. [2](#)

[36] Muhammad Tayyab Khan, Lequn Chen, Zane Yong, Jun Ming Tan, Wenhe Feng, and Seung Ki Moon. From drawings to decisions: A hybrid vision-language framework for parsing 2d engineering drawings into structured manufacturing knowledge. *arXiv preprint arXiv:2506.17374*, 2025.

[37] Muhammad Tayyab Khan, Zane Yong, Lequn Chen, Wenhe Feng, Nicholas Yew Jin Tan, and Seung Ki Moon. A multi-stage hybrid framework for automated interpretation of multi-view engineering drawings using vision language model. *arXiv preprint arXiv:2510.21862*, 2025. [2](#)

[38] Omar Khattab and Matei Zaharia. Colbert: Efficient and effective passage search via contextualized late interaction over bert. In *Proceedings of the 43rd International ACM SIGIR conference on research and development in Information Retrieval*, pages 39–48, 2020. [2](#)

[39] Geewook Kim, Teakgyu Hong, Moonbin Yim, Jinyoung Park, Jinyeong Yim, Wonseok Hwang, Sangdoo Yun, Dongyoon Han, and Seunghyun Park. Donut: Document understanding transformer without ocr. *arXiv preprint arXiv:2111.15664*, 7(15):2, 2021. [2](#)

[40] Patrick Lewis, Ethan Perez, Aleksandra Piktus, Fabio Petroni, Vladimir Karpukhin, Naman Goyal, Heinrich Küttler, Mike Lewis, Wen-tau Yih, Tim Rocktäschel, et al. Retrieval-augmented generation for knowledge-intensive nlp tasks. *Advances in neural information processing systems*, 33:9459–9474, 2020. [2](#)

[41] Tsung-Yi Lin, Michael Maire, Serge Belongie, Lubomir Bourdev, Ross Girshick, James Hays, Pietro Perona, Deva Ramanan, C. Lawrence Zitnick, and Piotr Dollár. Microsoft coco: Common objects in context, 2015. [2](#)

[42] Haotian Liu, Chunyuan Li, Qingyang Wu, and Yong Jae Lee. Visual instruction tuning, 2023. [2](#)

[43] Chuwei Luo, Yufan Shen, Zhaoqing Zhu, Qi Zheng, Zhi Yu, and Cong Yao. Layoutlm: Layout instruction tuning with large language models for document understanding. In *Proceedings of the IEEE/CVF conference on computer vision and pattern recognition*, pages 15630–15640, 2024. [2](#)

[44] Peter Rex Massingham. Measuring the impact of knowledge loss: a longitudinal study. *Journal of Knowledge Management*, 22(4):721–758, 2018. [1](#)

[45] Minesh Mathew, Viraj Bagal, Rubén Tito, Dimosthenis Karatzas, Ernest Valveny, and CV Jawahar. Infographiccvqa. In *Proceedings of the IEEE/CVF Winter Conference on Applications of Computer Vision*, pages 1697–1706, 2022. [2](#)

[46] Alexander Most, Joseph Winjum, Manish Bhattacharai, Shawn Jones, Nishath Rajiv Ranasinghe, Ayan Biswas, and Dan O’Malley. Lost in ocr translation? vision-based approaches to robust document retrieval. In *Proceedings of the 2025 ACM Symposium on Document Engineering*, pages 1–10, 2025. [1](#)

[47] T Sreekanta Murthy and JS Arora. A survey of database management in engineering. *Advances in Engineering Software* (1978), 7(3):126–132, 1985. [1](#)

[48] Srirama Nakshathri, Pratyusha Rasamsetty, and Deepak Kumar. Automating scale extraction from engineering drawings: A multi-step vision and text approach. In *2025 IEEE 15th Annual Computing and Communication Workshop and Conference (CCWC)*, pages 00945–00951, 2025. [2](#)

[49] Michal Ondrejcek, Jason Kastner, Rob Kooper, and Peter Bajcsy. Information extraction from scanned engineering drawings. *National Center for Supercomputing Applications, University of Illinois at Urbana-Champaign, Image Spatial DataAnalysis Group*, 1, 2009. [1](#)

[50] OpenAI. Gpt-5 technical report, 2025. Available at <https://openai.com/research/>. [2](#)

[51] OpenAI, :, Aaron Hurst, Adam Lerer, Adam P. Goucher, et al. Gpt-4o system card, 2024. [4](#)

[52] Birgit Pfitzmann, Christoph Auer, Michele Dolfi, Ahmed S. Nassar, and Peter Staar. Doclaynet: A large human-annotated dataset for document-layout segmentation. In *Proceedings of the 28th ACM SIGKDD Conference on Knowledge Discovery and Data Mining*, page 3743–3751. ACM, 2022. [2](#)

[53] Bryan A. Plummer, Liwei Wang, Chris M. Cervantes, Juan C. Caicedo, Julia Hockenmaier, and Svetlana Lazebnik. Flickr30k entities: Collecting region-to-phrase correspondences for richer image-to-sentence models, 2016. [2](#)

[54] Yingqi Qu, Yuchen Ding, Jing Liu, Kai Liu, Ruiyang Ren, Wayne Xin Zhao, Daxiang Dong, Hua Wu, and Haifeng Wang. Rocketqa: An optimized training approach to dense passage retrieval for open-domain question answering, 2021. [2](#)

[55] Alec Radford, Jong Wook Kim, Chris Hallacy, Aditya Ramesh, Gabriel Goh, Sandhini Agarwal, Girish Sastry, Amanda Askell, Pamela Mishkin, Jack Clark, Gretchen Krueger, and Ilya Sutskever. Learning transferable visual models from natural language supervision, 2021. [2, 4](#)

[56] Stephen Robertson, Hugo Zaragoza, et al. The probabilistic relevance framework: Bm25 and beyond. *Foundations and Trends® in Information Retrieval*, 3(4):333–389, 2009. [2](#)

[57] Martin P Robillard. Turnover-induced knowledge loss in practice. In *Proceedings of the 29th ACM Joint Meeting on European Software Engineering Conference and Symposium on the Foundations of Software Engineering*, pages 1292–1302, 2021. [1](#)

[58] J. J. Rocchio. Relevance feedback in information retrieval. In *The Smart retrieval system - experiments in automatic document processing*, pages 313–323. Englewood Cliffs, NJ: Prentice-Hall, 1971. [2](#)

[59] Keshav Santhanam, Omar Khattab, Jon Saad-Falcon, Christopher Potts, and Matei Zaharia. Colbertv2: Effective and efficient retrieval via lightweight late interaction. *arXiv preprint arXiv:2112.01488*, 2021. [2](#)

[60] Tao Shen, Guodong Long, Xiubo Geng, Chongyang Tao, Yibin Lei, Tianyi Zhou, Michael Blumenstein, and Dixin

Jiang. Retrieval-augmented retrieval: Large language models are strong zero-shot retriever. In *Findings of the Association for Computational Linguistics: ACL 2024*, pages 15933–15946, Bangkok, Thailand, 2024. Association for Computational Linguistics. [2](#)

[61] Noah Siegel, Zachary Horvitz, Roie Levin, Santosh Divvala, and Ali Farhadi. Figureseer: Parsing result-figures in research papers. In *European Conference on Computer Vision*, pages 664–680. Springer, 2016. [2](#)

[62] Brandon Smock, Rohith Pesala, and Robin Abraham. Pubtables-1m: Towards comprehensive table extraction from unstructured documents, 2021. [2](#)

[63] Mupparaju Sohan, Thotakura Sai Ram, and Ch Venkata Rami Reddy. A review on yolov8 and its advancements. In *International Conference on Data Intelligence and Cognitive Informatics*, pages 529–545. Springer, 2024. [2](#), [4](#)

[64] Weiwei Sun, Lingyong Yan, Xinyu Ma, Shuaiqiang Wang, Pengjie Ren, Zhumin Chen, Dawei Yin, and Zhaochun Ren. Is chatgpt good at search? investigating large language models as re-ranking agents, 2024. [2](#)

[65] Gemma Team, Aishwarya Kamath, Johan Ferret, Shreya Pathak, Nino Vieillard, Ramona Merhej, Sarah Perrin, Tatiana Matejovicova, Alexandre Ramé, Morgane Rivière, et al. Gemma 3 technical report. *arXiv preprint arXiv:2503.19786*, 2025. [2](#)

[66] Javier Villena Toro, Anton Wiberg, and Mehdi Tarkian. Optical character recognition on engineering drawings to achieve automation in production quality control. *Frontiers in manufacturing technology*, 3:1154132, 2023. [2](#)

[67] Ellen M Voorhees, Donna K Harman, et al. *TREC: Experiment and evaluation in information retrieval*. The MIT Press, 2005. [2](#)

[68] Alisha A Waller, Joseph M LeDoux, and Wendy C Newstetter. What makes an effective engineering diagram? a comparative study of novices and experts. In *2013 ASEE Annual Conference & Exposition*, pages 23–1366, 2013. [1](#)

[69] Bin Xiao, Haiping Wu, Weijian Xu, Xiyang Dai, Houdong Hu, Yumao Lu, Michael Zeng, Ce Liu, and Lu Yuan. Florence-2: Advancing a unified representation for a variety of vision tasks. In *Proceedings of the IEEE/CVF Conference on Computer Vision and Pattern Recognition*, pages 4818–4829, 2024. [2](#)

[70] Yiheng Xu, Minghao Li, Lei Cui, Shaohan Huang, Furu Wei, and Ming Zhou. Layoutlm: Pre-training of text and layout for document image understanding. In *Proceedings of the 26th ACM SIGKDD international conference on knowledge discovery & data mining*, pages 1192–1200, 2020. [2](#)

[71] Yang Xu, Yiheng Xu, Tengchao Lv, Lei Cui, Furu Wei, Guoxin Wang, Yijuan Lu, Dinei Florencio, Cha Zhang, Wanxiang Che, et al. Layoutlmv2: Multi-modal pre-training for visually-rich document understanding. *arXiv preprint arXiv:2012.14740*, 2020. [2](#)

[72] Zhenyu Yang, Dizhan Xue, Shengsheng Qian, Weiming Dong, and Changsheng Xu. Ldre: Llm-based divergent reasoning and ensemble for zero-shot composed image retrieval. In *Proceedings of the 47th International ACM SIGIR conference on research and development in information retrieval*, pages 80–90, 2024. [2](#)

[73] Rui Yao, Xin Cheng, Zhilei Hui, Zexin Li, and Zhaoe Min. Intelligent reading for multi-scale engineering drawings based on adaptive object detection and optical character recognition. In *9th International Conference on Industrial Engineering and Applications*, pages 1484–1492, 2022. [2](#)

[74] Xinlu Zhang, Yujie Lu, Weizhi Wang, An Yan, Jun Yan, Lianke Qin, Heng Wang, Xifeng Yan, William Yang Wang, and Linda Ruth Petzold. Gpt-4v (ision) as a generalist evaluator for vision-language tasks. *arXiv preprint arXiv:2311.01361*, 2023. [2](#)

[75] Lianmin Zheng, Wei-Lin Chiang, Ying Sheng, Siyuan Zhuang, Zhanghao Wu, Yonghao Zhuang, Zi Lin, Zhuohan Li, Dacheng Li, Eric P. Xing, Hao Zhang, Joseph E. Gonzalez, and Ion Stoica. Judging llm-as-a-judge with mt-bench and chatbot arena, 2023. [2](#)

A. Additional Ablations

A.1. Zero-Shot Document Classification

The first step in our framework was to distinguish between engineering drawings and textual documents. We evaluated four approaches on the withheld golden test set of 1,500 files. Baseline methods performed poorly: the NLP-based BART-large model achieved only 49.1% accuracy overall, with near-zero recall on drawings (0.8%) and a corresponding F1 score of just 1.5%. A heuristics-based baseline, implemented as a logistic regression classifier over structural features (e.g., edges, lines, shapes), performed similarly with 48.4% accuracy, achieving moderate performance on drawings ($F1 = 0.61$) but very low performance on documents ($F1 = 0.24$).

In contrast, vision-based methods provided a substantial improvement. CLIP achieved 93.3% accuracy, with balanced performance across both categories ($F1 = 0.93$ for documents and 0.93 for drawings). When combined with heuristics, CLIP’s performance further improved, reaching 94.5% overall accuracy, with F1 scores of 0.94 for documents and 0.95 for drawings, the best results across all approaches. These results confirm that multimodal, vision-driven zero-shot methods are highly effective for large-scale filtering of engineering archives, outperforming both NLP and heuristic baselines by a wide margin (Table 7, Figure 6).

Table 7. Zero-shot performance (drawing vs. document) on the withheld golden test set (1500 files). Best values per column are in **bold**.

Model	Type	Prec.	Rec.	F1	Acc.
Heuristics only	Drawing	0.490	0.808	0.610	0.484
	Document	0.455	0.160	0.237	
BART-large	Drawing	0.240	0.008	0.015	0.491
	Document	0.496	0.975	0.657	
CLIP	Drawing	0.922	0.945	0.934	0.933
	Document	0.944	0.920	0.932	
CLIP+Heuristics	Drawing	0.919	0.977	0.947	0.945
	Document	0.976	0.913	0.944	

A.2. Information Detection

Accurate region detection is a prerequisite for all downstream OCR and identifier extraction. We therefore evaluated a range of modern object-detection models on our engineering-drawing detection benchmark. Our primary detector is YOLOv8-S, trained on 500 annotated drawings and evaluated on a held-out set of 250 unseen drawings. We use YOLOv8-S because it provides an excellent accuracy-latency trade-off: as shown in Table 8, YOLOv8-S

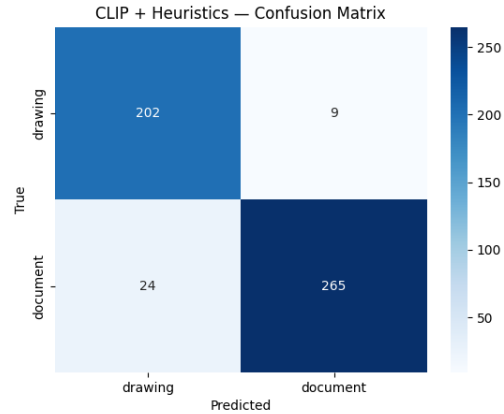


Figure 6. Confusion matrix for the drawing vs. document classification task. Values are normalized by row. (Clip + Heuristics)

matches the accuracy of newer variants such as YOLOv11-S while running substantially faster.

To assess robustness, we ablate YOLOv8-S against (i) other YOLO families (YOLOv5-S, YOLOv10-S, YOLOv11-S) and (ii) state-of-the-art transformer-based detectors (RT-DETR, Faster R-CNN, RetinaNet). YOLOv8-S achieves the highest mAP@0.5:0.95 among all real-time models, with competitive precision/recall and very low latency, making it well suited for high-volume archival processing where millions of pages must be scanned quickly. Reliable detection ensures that subsequent OCR operates on clean, semantically meaningful regions (e.g., title blocks, revision tables, parts lists), which directly improves identifier normalization and downstream retrieval accuracy.

B. Evaluation Metrics

For clarity and reproducibility we define all metrics in this section.

B.1. Detection & Classification Metrics

We evaluated the performance of our vision pipeline against a manually annotated subset of the corpus using standard classification metrics.

Accuracy. Overall accuracy measures the proportion of correctly classified files:

$$\text{Acc} = \frac{1}{N} \sum_{i=1}^N \mathbf{1}\{\hat{y}^{(i)} = y^{(i)}\}, \quad (1)$$

where $y^{(i)}$ is the ground-truth label for file i , $\hat{y}^{(i)}$ is the predicted label, and $\mathbf{1}\{\cdot\}$ is the indicator function.

Table 8. Comparison of detection models on the withheld engineering drawing test dataset. All accuracy values are percentages; latency measured in milliseconds per image.

Model	mAP@0.5:0.95	Recall	Precision	Params (M)	GFLOPs	Latency (ms)
YOLOv5-S	87.94	90.56	97.36	9.12	24.05	2.68
YOLOv8-S	89.50	92.61	96.51	11.14	28.66	5.16
YOLOv10-S	85.17	88.89	93.54	8.07	24.79	92.23
YOLOv11-S	89.50	92.13	95.83	9.43	21.56	81.37
Faster R-CNN (R-50 FPN)	78.11	90.88	89.69	41.0	180.3	45.10
RetinaNet (R-50 FPN)	55.55	90.58	79.43	36.4	150.2	33.00
RT-DETR-L	88.51	93.28	96.95	32.82	108.0	27.87

Precision and Recall. For each class $k \in \{\text{drawing, document}\}$, we define true positives (TP_k), false positives (FP_k), and false negatives (FN_k). Precision and recall are then:

$$\text{Prec}_k = \frac{TP_k}{TP_k + FP_k}, \quad (2)$$

$$\text{Rec}_k = \frac{TP_k}{TP_k + FN_k}. \quad (3)$$

F1 Score. The F1 score is the harmonic mean of precision and recall:

$$F1_k = \frac{2 \cdot \text{Prec}_k \cdot \text{Rec}_k}{\text{Prec}_k + \text{Rec}_k}. \quad (4)$$

Macro Average. To summarize performance across both classes, we report the macro-average of each metric:

$$\text{Macro-}M = \frac{1}{2} \sum_{k \in \{\text{drawing, document}\}} M_k, \quad (5)$$

where M_k denotes precision, recall, or F1 for class k .

B.2. Retrieval Metrics

For the end-to-end retrieval benchmark (Table 3), we evaluate each system using standard information-retrieval metrics adapted to our graded relevance scheme (0/1/2). Because many computer vision readers may be less familiar with these metrics, we briefly define them here.

nDCG@3. Normalized Discounted Cumulative Gain measures how well a ranked list places highly relevant items near the top. For a query q :

$$\text{DCG@3}(q) = \sum_{i=1}^3 \frac{\ell(q, d_i)}{\log_2(i+1)}, \quad (6)$$

$$\text{nDCG@3}(q) = \frac{\text{DCG@3}(q)}{\text{IDCG@3}(q)}, \quad (7)$$

where IDCG@3 is the maximum achievable DCG for that query.

MAP@3. Mean Average Precision evaluates how consistently relevant items appear across the top-3 positions:

$$\text{AP@3}(q) = \frac{1}{R(q)} \sum_{i=1}^3 \text{Prec}@i(q) \mathbf{1}\{\ell(q, d_i) > 0\}, \quad (8)$$

where $R(q)$ is the number of relevant items. We report two versions:

- **MAP@3(≥1)** — counts any relevance $\ell > 0$,
- **MAP@3(=2)** — requires the highest relevance grade.

Precision@3 and Recall@3. Precision@3 measures the fraction of top-3 items that are relevant; Recall@3 measures the fraction of all relevant items retrieved:

$$\text{P@3}(q) = \frac{1}{3} \sum_{i=1}^3 \mathbf{1}\{\ell(q, d_i) > 0\}, \quad (9)$$

$$\text{R@3}(q) = \frac{1}{R(q)} \sum_{i=1}^3 \mathbf{1}\{\ell(q, d_i) > 0\}. \quad (10)$$

Success@3. Success@3 indicates whether at least one relevant item appears in the top-3:

$$\text{Succ@3}(q) = \mathbf{1}\left\{ \max_{i \leq 3} \ell(q, d_i) \geq 1 \right\}. \quad (11)$$

Aggregation. All metrics are computed per query and then averaged across the 375 benchmark queries (150 vision-only, 150 NLP-only, 75 multimodal). We report mean \pm 95% confidence intervals over the per-query scores.

C. Baseline Models and Prompting Protocols

To ensure fair and reproducible comparison across systems, we document all baseline models, prompts, and decoding settings used in the retrieval experiments. All systems—including BLUEPRINT—were evaluated under the same input constraints and returned their top- k ranked items for every query.

C.1. A. Model Suite

We evaluate six state-of-the-art vision–language models (VLMs) alongside our proposed BLUEPRINT system:

- **LLaMA 3.2 Vision 11B** (full-page vision encoder + LLaMA-3.2 decoder)
- **Llama-4-Scout 17B** (OCR-heavy retrieval-oriented model)
- **LLAVA-1.6-Mistral 7B**
- **PaLI-Gemma 2 3B**
- **Pixtral 12B**
- **Phi-3.5-Vision** (ablations only; struggled with full-page inputs)
- **BLUEPRINT** (ours: region-aware pipeline + hybrid retrieval)

All models were run exactly as released by their maintainers, with no fine-tuning, task-specific adapters, or retrieval-engine modifications. Models were limited to the same maximum input resolution and were given access only to full-page image renders (no region hints, no bounding boxes, and no OCR text unless produced by the model itself).

C.2. Prompting Protocol

To avoid inadvertently favoring any model family, all baselines received the same natural-language retrieval prompt for each query, presented in Figure 7.

No system was allowed to “cheat” by inspecting folder paths, filenames outside the render, or metadata unavailable to others.

Constraint handling. Baselines were not provided any additional engineering-domain heuristics. For example, a request for “drawings size E” must be inferred purely from OCR or visual inspection, not any model-specific rules. This ensured that improvements arise from BLUEPRINT’s structured extraction and not from query leakage or handcrafted logic.

C.3. Decoding and Search Parameters

All systems used deterministic decoding:

- `do_sample = False` (greedy decoding; no sampling),
- `top_p = 1.0` (default, unused when `do_sample = False`),
- `max_new_tokens = 512` per page.

Image preprocessing. All baselines received:

- full-page (PNG/PDF) renders at fixed resolution (2048 px max side),
- no region crops,
- no pre-extracted title blocks, revision tables, or parts lists.

This ensured that any advantage from structured region extraction originates from BLUEPRINT itself.

Table 9. Human evaluation success at $top_k=1$ (Succ@1): mean \pm 95% CI over queries. Three raters (1 expert, 2 trained raters). 50 queries: 25 vision, 15 NLP, 10 multi-modal.

System	All	Vision	NLP	MM
Llama-3.2-11B-V	0.49 ± 0.14	0.33 ± 0.19	0.73 ± 0.20	0.50 ± 0.30
L4-Scout-17B	0.43 ± 0.14	0.36 ± 0.18	0.29 ± 0.21	0.80 ± 0.25
LLava-1.6-M	0.31 ± 0.12	0.36 ± 0.18	0.29 ± 0.21	0.20 ± 0.25
PaLI-Gemma-2-3B	0.18 ± 0.11	0.24 ± 0.16	0.13 ± 0.17	0.10 ± 0.15
Pixtral-12B	0.35 ± 0.14	0.24 ± 0.16	0.57 ± 0.29	0.33 ± 0.33
Blueprint	0.74 ± 0.12	0.72 ± 0.18	0.60 ± 0.27	1.00 ± 0.00

C.4. Blueprint Query Pipeline

For completeness, BLUEPRINT received the same text query but used its internal multimodal pipeline:

1. zero-shot document/drawing classification,
2. YOLOv8-S region detection,
3. VLM-based OCR for title blocks, parts lists, revision tables, etc.,
4. identifier normalization (DWG number, rev, facility code),
5. hybrid sparse+dense retrieval with region-aware reranking.

C.5. Fairness Considerations

To ensure no model was advantaged:

- All models saw the same query wording.
- All models received identical image renders.
- No model received privileged internal metadata.
- All were capped at three final ranked outputs.
- All judgments (human+LLM) were done on anonymized outputs.

This evaluation design emphasizes retrieval ability, not language-model fluency or caption length.

D. Human Evaluation

System rankings. Each system’s relevance score was averaged across human raters, and per-query nDCG@1 was computed with bootstrap 95% confidence intervals. Table 9 shows that BLUEPRINT achieves the highest human-validated retrieval accuracy, with mean nDCG@1 = **0.74 ± 0.12** . The strongest baseline, Llama-3.2-11B-Vision, reaches 0.49 ± 0.14 , followed by Llama-4-Scout-17B (0.43 ± 0.14).

Full-page VLMs such as Pixtral-12B (0.35 ± 0.14) and PaLI-Gemma-2-3B (0.18 ± 0.11) underperform substantially, highlighting that generic vision–language reasoning does not transfer well to engineering diagrams or multi-region technical documents. Blueprint’s margin is widest on multi-modal queries (1.00 ± 0.00), where accurate integration of layout, identifiers, and text is essential.

You are an ingestion agent for engineering archives. You will be shown ONE page as an image. Your job has THREE steps:

(1) CLASSIFY

Decide the document type. Choose exactly ONE from:
 - ENGINEERING_DRAWING
 - POLICY
 - PROCEDURE
 - OTHER

(2) EXTRACT

Depending on the type, extract strongly structured content:

A. If it is an ENGINEERING_DRAWING:

- drawing_number: the main drawing / print / figure / doc number in the title block
- title_block_text: all text in the title block
- revision_block_text: all text in the revision/change block
- parts_list_or_bom: any tabular/parts list, row by row
- notes: general notes, welding/material notes, callouts
- ALSO output the full plain-text reading of the entire page

B. If it is a POLICY:

- policy_id or number if present
- title / subject
- section_headings (in order)
- body_text (full text)
- tables (if visible)

C. If it is a PROCEDURE:

- procedure_id or number if present
- title
- steps (numbered or bulleted) in order
- prerequisites / scope / purpose if visible
- tables / forms if visible
- body_text (full text)

D. If it is OTHER:

- title or top heading if any
- body_text (full text)
- tables if visible

(3) OUTPUT

Return ONLY JSON in this shape:

```
{
  "doc_type": "<ENGINEERING_DRAWING | POLICY | PROCEDURE | OTHER>",
  "text": "<full-page plain text with line breaks>",
  "drawing_fields": {
    "drawing_number": "...",
    "title_block_text": "...",
    "revision_block_text": "...",
    "parts_list_or_bom": "...",
    "notes": "..."
  },
  "policy_fields": {
    "policy_id": "...",
    "title": "...",
    "section_headings": "...",
    "tables": "..."
  },
  "procedure_fields": {
    "procedure_id": "...",
    "title": "...",
    "steps": "...",
    "tables": "..."
  }
}
```

Figure 7. Prompt used for full-page ingestion and structured extraction for all baseline models.

D.1. Inter-Rater Reliability

To quantify the consistency of human annotations, we measured pairwise and multi-rater agreement across the three evaluators (1 expert, 2 trained raters) using the same graded relevance labels (0/1/2) used throughout the benchmark.

Pairwise agreement. Across the overlapping items for each pair of raters, we observe strong alignment:

- **rater 1 vs. rater 2:** 324 overlapping items, 72.8% raw agreement, Cohen's $\kappa=0.36$ (unweighted), and quadratic-weighted $\kappa_w=0.52$.

- **rater 1 vs. rater 3:** 300 overlapping items, 76.7% raw agreement, Cohen’s $\kappa=0.51$, and $\kappa_w=0.69$.
- **rater 2 vs. rater 3:** 324 overlapping items, 77.2% raw agreement, Cohen’s $\kappa=0.36$, and $\kappa_w=0.49$.

Quadratic-weighted kappas between 0.49–0.69 indicate *moderate to strong* agreement for a 3-level ordinal scale, consistent with expectations for fine-grained 0/1/2 relevance judgments over heterogeneous engineering documents.

Model-level consistency. Per-variant agreement is generally high across raters (typically 0.74–0.89). BLUEPRINT shows somewhat lower pairwise agreement (0.42–0.63), not due to inconsistency, but because it more frequently surfaces borderline-relevant cases (e.g., multiple contextually plausible drawings), which require careful disambiguation. This is consistent with the system achieving the highest recall-oriented and multi-modal retrieval performance.

Multi-rater reliability. Considering all three raters simultaneously, 290 items were annotated by all raters. Full agreement occurred on 63.8% of items, and Fleiss’ $\kappa=0.40$, again indicating moderate agreement across the 0/1/2 relevance scale.

Together, these results demonstrate that the human annotations used to validate BLUEPRINT are consistent and reliable across raters, and that the graded relevance scheme produces stable judgments despite the diversity of technical documents involved.

E. LLM as Judge

To evaluate models and reduce human workload in a real-world engineering setting, we implement a framework for “LLM as judge” in both an arena setting and a statistical analysis. These judges and statistics are discussed in Section 5.2 of the main paper.

Decoding settings. All LLM judges used fully deterministic decoding to ensure strict reproducibility. We set: `temperature = 0`, `top_p = 1`, and `max_tokens = 4000` for Arena judgments (with effectively unlimited tokens for the JSON scoring task). No sampling, nucleus randomness, or system-level stochasticity was used beyond the randomized A/B model order. This guarantees that all variation in judgments is due solely to model behavior, not decoding noise

Why LLM as Judge? Engineering archives at academic and industrial facilities contain hundreds of thousands of unlabeled files. Full human judgment is infeasible at scale: manually labeling the 375-query \times 6-model matrix would require $\sim 6,300$ individual relevance annotations, which is infeasible to perform manually. “LLM as judge” reduces this cost substantially, while maintaining human-level reliability through a hybrid LLM–human framework.

Arena. Three judges (GPT-5, Llama-3.2, Mistral-7B; for ablations, Phi-3.5 replaced Mistral-7B but struggled on full-page prompts). To ensure fairness, the order of systems was randomized: BLUEPRINT appeared as “System A” exactly 50% of the time and “System B” the other 50%. This mitigates positional bias, where a judge, if uncertain, may default to the first system. All judges received identical prompts and decoding settings.

Figure 8 shows the exact prompt used in the arena evaluation, while Table 10 presents GPT-5’s judgments for the query q = “drawings size E and only 1 sheet”.

Retrieval scoring. In a similar vein, each LLM judge was given an anonymous model along with its $\text{top-}k = 3$ retrieved documents and asked to score each document *independently* on a 3-point scale (0/1/2). All judges received identical prompting, token limits, and formatting to ensure consistency. Importantly, retrieval scoring was always conducted *one model at a time*: each judge saw only a single system’s top- k results for independent scoring. We initially experimented with presenting multiple systems simultaneously in a ranked list, but this introduced strong positional bias (items shown earlier tended to receive higher scores, regardless of model). The final protocol therefore uses single-system evaluation to eliminate position-induced preference.

Figure 9 shows the verbatim prompt given to each judge. Table 11 illustrates a representative example of this scoring protocol. Interestingly, in this case BLUEPRINT’s rank-1 result received a score of 1, whereas several baselines obtained a 2 at rank 1. However, BLUEPRINT achieved scores of 2 at both rank 2 and rank 3, while competing models typically returned off-type or irrelevant items beyond their first result. This highlights the advantage of evaluating all top- k items independently: although some models occasionally surface a strong item at rank 1, BLUEPRINT demonstrates stronger overall retrieval quality across the ranked list.

F. Benchmark Query Set

Our retrieval benchmark consists of 375 anonymized queries designed to span the full range of information needs encountered in large engineering archives. The queries were constructed to be realistic, diverse, and balanced across modalities. Each query is expressed in natural language, and many contain multiple constraints or anchors (e.g., material type, revision, component count, date, hazard category, naming pattern, or facility/project reference).

Query distribution. The 375 queries are evenly partitioned into three categories:

- **150 Vision-only:** Targeting engineering drawings exclusively. These include geometric constraints (e.g., drawing size, sheet count), structural cues (e.g., electrical vs. mechanical vs. civil), component-based cues (e.g., part counts or manufacturer hints), and revision/identifier patterns.

You are an objective judge for retrieval from a legacy engineering archive.

You will receive:

- A user query Q. Q may target drawings, documents, or BOTH (multimodal).
- Two anonymous systems (System A and System B). Each system returns up to 5 ranked items.
- Each returned item may be a DRAWING or a DOCUMENT; items include minimal metadata (e.g., drawing number, sheet, rev, material, facility/building, parts count, doc id/code, title, author, date).

Your task:

Choose which system is better for this query: A, B, or tie.

Judging rules (apply in order):

A. INTENT MATCH

- If Q names an identifier (e.g., drawing "drawing num", code xyz), systems that return the exact target at rank 1 (or near the top) should be preferred.
- If Q requires BOTH (asks for a procedure/policy/document AND a drawing), prefer systems whose top results collectively satisfy BOTH in the top-5.
- If Allowed types are provided, treat them as a hard constraint.

B. CONSTRAINT SATISFACTION

- Prefer items that satisfy secondary constraints (building, material, rev, sheet, parts count, facility, date, author, vendor).

C. RANKING QUALITY

- Correct items appearing higher are better than the same items lower.
- Penalize unrelated items, hallucinated IDs, or near-duplicate items.

D. MULTIMODAL PAIRING (when Q is BOTH)

- Extra credit when both modalities appear with consistent anchors.
- Partial satisfaction is strictly worse than full satisfaction.

Tie-breaking (only if needed):

- 1) More exact anchor matches.
- 2) More constraints satisfied.
- 3) Higher useful density in ranks 1--2.
- 4) Fewer unrelated items.

Output STRICTLY JSON ONLY:

```
{  
  "winner": "A" | "B" | "tie",  
  "explanation": "brief reason (1-2 sentences)"  
}
```

Figure 8. Arena-style prompt used for the LLM-as-judge comparison between two anonymous retrieval systems. All judges and models received the identical prompt; only the system outputs were permuted.

- **150 Document-only:** Targeting policies, procedures, manuals, and other text-heavy technical documents. These queries emphasize temporal constraints, naming conventions, hazard references, authorship cues, operational context, and external standards.
- **50 BOTH (Multimodal):** Requiring a *pair* of items, a document and a drawing, that jointly satisfy a shared anchor such as a common identifier, project code, building reference, or cross-linked operational procedure. These represent realistic workflows in engineering environments where drawings and procedures must be consulted together.

Motivation and design goals. The query set is intended to:

- capture the heterogeneity of real-world engineering information needs,
- require multimodal understanding (visual + textual) for a substantial portion of the benchmark,
- stress-test both OCR quality and normalization robustness,
- include queries with varying specificity (broad, narrow, multi-constraint),
- and avoid any bias toward a particular retrieval model's strengths.

Anonymization. All identifiers, including drawing numbers, facility codes, building identifiers, document names, and organization-specific prefixes, were replaced with abstracted tokens or structurally similar placeholders. The semantic structure of each query was preserved, but no pro-

Query: “drawings size E and only 1 sheet”			
Model A	Model B	Winner	Judge Explanation
Blueprint	Llama-3.2-Vision	A	Blueprint returns engineering drawings matching <i>SIZE E</i> and <i>1 of 1 sheets</i> , while B returns off-type documents.
llava-v1.6-mistral-7b-hf	Blueprint	B	Blueprint returns drawings satisfying size and sheet constraints; A returns mostly policies (off-type).
paligemma2-3b-mix-224	Blueprint	B	B returns engineering drawings, including <i>SIZE E, 1-sheet</i> items; A returns documents violating allowed types.
pixtral-12b	Blueprint	B	B provides engineering drawings matching the constraints; A returns documents only.
Llama-4-Scout-17B-Instruct	Blueprint	B	Blueprint returns drawings with rank 2–3 satisfying <i>SIZE E</i> and <i>1-sheet</i> ; A returns only documents.

Table 10. Arena-style LLM-judge comparisons for the query “drawings size E and only 1 sheet.” All judgments were produced by the GPT-5 arena judge. Across all baselines, BLUEPRINT consistently satisfies the ENGINEERING_DRAWING type constraint and returns valid size E, 1-sheet drawings near the top of its ranking.

You are scoring engineering retrieval results for a legacy archive.

You will be given:

- the user query (it may ask for a DRAWING, a DOCUMENT, or BOTH)
- optional Allowed types (ENGINEERING_DRAWING, POLICY, PROCEDURE)
- up to 3 ranked results from ONE system

Each result includes: rank (1 is best), item_id, kind (DRAWING or DOCUMENT), and an OCR text snippet (may include drawing numbers, revs, sheets, WBS/building, materials, authors, dates, parts lists, etc.).

Your task:

Score EVERY result independently using the 0/1/2 scale:

0 = not relevant or clearly wrong

1 = partially relevant (some match, incomplete)

2 = fully relevant / excellent answer to the query

Rules:

- Anchors (IDs, codes) strongly support score 2.
- Slight OCR noise is acceptable.
- If a query uses negation (e.g., \no parts list”), violating items score 0.
- If unclear, be conservative (0 or 1).

Modality and constraints:

- Allowed types are a hard constraint.
- If query asks for DRAWING, score drawing cues.
- If query asks for DOCUMENT, score document cues.
- If BOTH, either modality can score 2.

Return STRICT JSON ONLY:

```
{
  "ratings": [
    {"item_id": "SYSTEM-RANK1", "score": 0 | 1 | 2},
    {"item_id": "SYSTEM-RANK2", "score": 0 | 1 | 2}
  ]
}
```

Figure 9. Prompt used for per-document relevance scoring in the LLM-as-judge statistical evaluation.

prietary or sensitive identifiers remain.

Ground-truth relevance. Each query is linked to one or more target items in the corpus, with a graded relevance score of 0/1/2. A relevance of 2 indicates a fully correct

and highly informative match; a score of 1 indicates a partial or weakly correct match; and a score of 0 denotes irrelevance. Target items were manually validated to ensure correctness and modality alignment (e.g., vision-only queries never specify document targets).

Query: “retrieve the instruction manual for dissolved oxygen sensors”		
Model	Scores (1/2/3)	Judge Explanation
Blueprint	1, 2, 2	Returns procedures/manual-like documents; rank-2 and rank-3 appear strongly relevant to dissolved oxygen sensors.
Llama-3.2-11B-Vision-Instruct	2, 0, 0	Rank-1 matches intent (procedure), but lower ranks are irrelevant or off-type.
llava-v1.6-mistral-7b-hf	0, 0, 0	Returns entirely irrelevant or off-type results; no clear procedural match.
paligemma2-3b-mix-224	2, 0, 0	Rank-1 is a correct procedure; ranks-2/3 do not relate to the query.
pixtral-12b	0, 2, 0	Rank-2 is a valid procedure/manual; the others are unrelated.
Llama-4-Scout-17B-16E-Instruct	2, 2, 0	Strong relevant matches at ranks-1 and 2; rank-3 unrelated.

Table 11. Per-document statistical scoring (0/1/2 relevance) for the query “retrieve the instruction manual for dissolved oxygen sensors.” Each LLM judge evaluated one model at a time using the scoring prompt in Figure 9. Higher scores correspond to closer alignment with procedural intent and allowed type (PROCEDURE).

Evaluation protocol. For each system and query, the top-3 retrieved items are judged independently (either by human annotators or by the LLM-judge framework described in Section 5.2). Metrics such as nDCG@3, MAP@3, P@3, R@3, and Success@3 are computed per query and then averaged over their respective groups (vision, document, and multimodal).

Representative examples. Table 12 shows anonymized examples capturing the range of query intents. These illustrate the diversity of constraints (quantitative, structural, operational, temporal) and the multimodal nature of the benchmark.

Table 12. Representative examples of the 375 retrieval queries used in the benchmark. All identifiers, drawing numbers, facility codes, and document names have been anonymized. Queries cover vision-only (drawings), document-only (policies/procedures), and BOTH (multimodal) intents.

Type	Representative Query (Anonymized)
VISION	“Find mechanical drawings that show parts weighing approximately 0.3 pounds.”
VISION	“Retrieve engineering drawings that are size E and contain only a single sheet.”
VISION	“Retrieve a drawing revised to version C that depicts an electrical line diagram without a parts list.”
VISION	“Find structural drawings related to the concrete portion of a facility, labeled with the building’s project code.”
VISION	“Retrieve drawings that contain more than 25 components and include manufacturer cues such as common industrial suppliers.”
DOCUMENT	“Retrieve a procedure involving coordination with a maintenance or operability manager.”
DOCUMENT	“Retrieve a procedure created in early February that follows the naming pattern ‘XYZ--1.2.3’.”
DOCUMENT	“Retrieve a lift-plan document that references use of an overhead bridge crane and inspection requirements.”
DOCUMENT	“Retrieve a policy covering hazards such as welding, hot work, insects/wildlife, and scaffolding controls.”
DOCUMENT	“Retrieve a policy prepared by an external organization and revised in the mid-2000s related to safety or compliance.”
BOTH	“Retrieve BOTH the access-control procedure for a target-transfer operation AND the associated concrete building plan drawing.”
BOTH	“Retrieve BOTH the facility document with identifier ending in ‘-AB01234’ AND the drawing whose title block includes the matching facility code.”
BOTH	“Retrieve BOTH the HVAC/mechanical drawing showing a drain line AND the companion ductwork document referenced by that design.”
BOTH	“Retrieve BOTH a policy with a specific project code AND the drawing whose title block displays the same project identifier.”
BOTH	“Retrieve BOTH a feeder-schedule document AND the site-utilities plan drawing referenced within it.”